Available online at www.sciencedirect.com

ScienceDirect

Energy Procedia 38 (2013) 474 – 481

Energy Procedia

SiliconPV: March 25-27, 2013, Hamelin, Germany

High volume pilot production of high efficiency PERC solar cells - Analysis based on device simulation

Torsten Weber[a]*, Gerd Fischer[a†], Alexander Oehlke[a], Christian Kusterer[a], Kerstin Strauch[a], Roman Schiepe[a], Maria Mühlbauer[a], Matthias Müller[a], Franziska Wolny[a], Rene Köhler[a], Günther Grupp-Mueller[b], Eric Schneiderlöchner[a], Karl Heinz Stegemann[a], Holger Neuhaus[a]

[a]*SolarWorld Innovations GmbH, Berthelsdorferstr. 111A, 09599 Freiberg, Germany*
[b]*SolarWorld Industries America, 25300 NW Evergreen Rd, Hillsboro, OR 97124, USA*

Abstract

In this work we compare experimental results of an industrial passivated emitter and rear cell (PERC [1]) high volume pilot line production in the SolarWorld Innovations technology center with a simulation model based on 2D Sentaurus Device Simulations [2]. The PERC solar cell design shows in a well-controlled experiment a 1.1% absolute higher median efficiency compared to the aluminium back surface field (Al-BSF) solar cell reference group. We derive a calibrated simulation model by the characterization of cells and test structures. We show that the simulation model reproduces well the measured I-V data. In consequence this enables us to estimate the solar cell performance when an applied process or silicon wafer parameters will be changed for further optimization. In the second part of this study we investigate the impact of front and rear side recombination on the solar cell parameters by simulation and sensitivity analysis. We show that the quality of the local BSF underneath the local rear contacts has an important impact on the electrical solar cell performance.

Keywords: PERC; Device Simulation; SolarWorld; Pilot Production

* Corresponding author. Tel.: +49-3731-301-4874; fax: +49-3731-301-1690.
E-mail address: Torsten.weber@sw-innovations.de.

† Corresponding author. Tel.: +49-3731-301-4592; fax: +49-3731-301-1690.
E-mail address: Gerd.Fischer@sw-innovations.de.

doi:10.1016/j.egypro.2013.07.306

1. Introduction

One of the most promising new silicon based solar cell concepts for implementation in existing production lines is the PERC structure. It has been proposed as a next possible step to enhance Czochralski-grown (Cz)-silicon as well as multi-crystalline silicon solar cell performance over the last years by different R&D institutions [3-11]. More recently also solar equipment supplying companies as well as solar cell manufacturers have published their efforts and successes to make the PERC solar cell concept a more cost effective, high yield, high power and high volume manufacturing silicon wafer based mass product [12-14]. In this work we will present experimental data of the pilot production in the SolarWorld Innovations (SWIN) technology center and results of device simulations based on Sentaurus Device [2] of the PERC cell design. During the pilot production we focused on the optimization of the solar cell efficiency as well as the optimization of the process capability of several process steps.

2. Experimental details

Our partly automated technology center consists of manufacturing scale process tools which are required for the pilot line production of the nowadays most common aluminium back surface field (Al-BSF) solar cell. The center also hosts process equipment of varying degree of large-scale production and automation for developing and evaluating next generation high efficiency solar cell concepts as also the PERC concept. We are able to control and optimize the solar cell process in a very short turnaround time due to our inline metrology and offline measurement tools located in close proximity to the pilot line. In this environment we developed and implemented over the last several months a PERC technology for Cz-silicon wafers.

A typically used wafer format was a 156.5x156.5 mm^2 pseudosquare *p*-type wafer with an as-cut thickness of 180 µm and 1-3 Ωcm base resistivity. Saw damage removal and texturing were done using alkaline solutions. The $POCl_3$ diffusion process was optimized in terms of production feasibility and high electrical performance (e.g. low recombination and good contact formation). Emitter saturation current density (J_{0e}) below 150 fA/cm^2 has been obtained by applying the method of Kane and Swanson [15]. A selective emitter was implemented to ensure a low contact resistance to the front side metallization. The rear side passivation stack was adjusted in respect of low surface recombination velocity S_{rear}, high internal reflection and thermal stability. The rear contacts were implemented with a local BSF underneath. In terms of contacting the emitter and base we used standard screen printing technologies (including solder pads) aiming high fill factors, very good cell interconnection and best module performance.

As a first step we developed and optimized several single process steps e.g. double sided-passivated lifetime samples, J_{0e} samples and implied open circuit voltage iV_{oc} samples which were thermally treated e.g. by the firing step. We tracked the parameter distribution of the process for instance over the boat position of the diffusion process. This enables us in an early phase to focus the optimization on the process implementation in a high scale production environment. Moreover, we obtained therefore a first set of data points for the specification of all important and critical processes. The next step was to combine the single process steps into the final process sequence. After first iterations we compared the PERC design with the Al-BSF solar cell concept in a well-controlled experiment. The results will be discussed in the next chapter and are the basis for the process specification. Over a period of 4 weeks we produced about 15,000 PERC solar cells. We monitored all important and critical process parameter by inline and offline metrology equipment. In order to test the individual PERC process steps regarding stability and robustness we calculated the process capability index C_{pK} defined as

$$C_{pK} = Min\left|\frac{Mean - USL}{3\times\sigma}, \frac{Mean - LSL}{3\times\sigma}\right|$$

with the mean value *Mean*, the upper and lower specification limit *USL* and *LSL* and the standard deviation σ. The C_{pK} describes the process variation relative to the specification limits. For instance a C_{pK} value of 1.33 means that 99,99% of the measured parameter are distributed within the specification limits. With this statistical method we were able to validate the critical process steps.

3. Results

3.1. Comparison of Al-BSF vs PERC cell concept

A well-controlled comparison of the standard manufacturing Al-BSF solar cell process and the PERC concept based on two randomized groups resulted in more than 5% relative cell efficiency improvement due to the PERC architecture. Table I shows the significant absolute differences of the electrical parameters of the Al-BSF and PERC cell groups.

Table I: Absolute difference of the PERC cell group compared to Al-BSF group based on two small randomized wafer groups (median value of 100 cells for each group).

ΔV_{oc} (mV)	ΔJ_{sc} (mA/cm^2)	ΔFF (%)	$\Delta S_{ser}LfDf$* (Ωcm^2)	$\Delta\eta$ (%)
+20	+1.5	-1.0	+0.1	+1.1

*$\Delta S_{ser}LfDf$ is the calculated series resistance from the light and dark IV curve

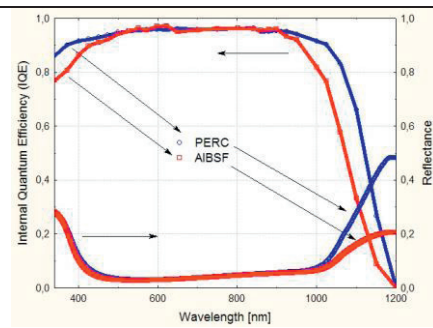

Fig. 1. Internal quantum efficiency (IQE) and reflectance comparison of PERC vs. AlBSF cell concept.

The improvement in the open circuit voltage (V_{oc}) and short circuit current (J_{sc}) is due to the excellent rear side passivation and emitter quality. An additional gain in J_{sc} is based on the enhanced internal reflection in the near infrared spectrum due to the rear dielectrical layer. Fig. 1 shows the internal quantum efficiency (IQE) and reflectance of a typical Al-BSF (red curve) and PERC (blue curve) solar cell. An increased series resistance and recombination losses contribute to the loss in fill factor and will be discussed in the simulation part.

The shown efficiency gain is above the break-even point based on internal cost of ownership calculations and therefore reveals the high potential of our PERC concept.

3.2. Pilot production

In a next step we moved our efforts towards running the PERC process sequence with increased volume through our pilot line. We could reproduce the high efficiencies and stabilize the process in a pilot phase over 4 weeks. In Fig. 2 we present the distribution of cell power of a volume of about 15,000 PERC solar cells based on wafer material which includes all sections of a standard Cz-crystal. This covers a base resistance range from 1 - 3 Ωcm as well as variation in oxygen and carbon concentration. A detailed analysis of the light induced degradation (LID) of this PERC design is published in *Wolny et al.*

[22]. The analysis of the process capability index of all critical process steps for instance the wet chemical cleaning, dielectric passivation or the local contact formation demonstrate the robustness of the used process sequence. The high efficiencies in combination with process capability indexes $C_{pK} > 1$ verify the applicability in high volume solar cell production lines.

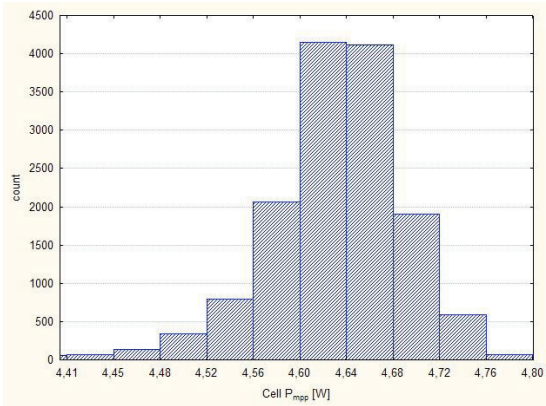

Fig. 2. Cell power distribution of the pilot production phase.

The subsequent loss analysis in chapter 4 is based on the results of this pilot phase.

3.3. Module results

Besides the important characterization of the PERC concept on cell level we investigated the performance of the solar modules made of 60 cells. To ensure the reliability, we employed the standard IEC 61215 test procedure including damp-heat, temperature-cycle, potential induced degradation (PID 300h @ 600 V, wet surface), humidity-freeze and hot-spot (IEC as well as UL) tests. The modules passed all IEC 61215 related tests with a power loss less than the tolerable 5%.

4. Loss analysis

4.1. Comparison of Al-BSF and PERC concept by simulation

We analyse our PERC concept with respect to the standard Al-BSF cell based on 2D Sentaurus Device Simulations [2]. The physical models described in reference [16] are applied. A loss analysis for both concepts is performed in order to understand the collected cell parameter of the Al-BSF vs. PERC comparison. To obtain the defect input parameter of the surface for our simulation, we measured the injection dependent lifetime of cleaned, double-sided passivated and fired lifetime samples. By fitting the obtained curve with a SRH model we extract the surface recombination parameters of electrons and holes $S_{n/p}$ and the effective surface recombination velocity S_{eff}. The dielectric fixed charge density (Q_f) of the passivation layer have been obtained by capacitive voltage (CV) measurements. For the bulk recombination dominated by boron-oxygen complexes we use the parametrization of Schmidt et al. [17]. The Emitter saturation current density (J_{0e} is below 150 fA/cm^2) has been obtained by applying the method of Kane and Swanson [15] to double-sided diffused and passivated lifetime samples.

In Table II we compare the simulated absolute differences between the Al-BSF and the PERC cells to the experimental median values. The excellent concordance demonstrates that our calibrated simulation

models are valid for both cell types. It could be confirmed that the improved V_{OC} and J_{SC} in our PERC cells are due to the lower recombination loss at the front and the rear side. Figure 3 shows a pareto graph of the relative recombination losses. It is well known that the performance of high efficiency Cz solar cells with passivated rear side is limited by the remaining rear surface recombination [18, 19]. The additional J_{SC} gain due to the enhanced internal reflection at the rear dielectric layer could be proven in ray tracing simulation.

Table II: Absolute difference of the PERC group compared to Al-BSF: experimental results vs. simulation.

	ΔV_{oc} (mV)	ΔJ_{sc} (mA/cm^2)	ΔFF (%)	$\Delta \eta$ (%)
experimental	+19.9	+1.47	-0.992	+1.10
simulation	+18.8	+1.46	-0.916	+1.06

The PERC concept has local rear contacts and therefore an intrinsic higher series resistance than the Al-BSF concept with a fully contacted rear side. However, the lower *FF* of the PERC cells cannot be completely explained by the higher series resistance. The *FF* is also strongly influenced by the injection dependence of the SRH recombination in the base. The Pareto graph for the recombination losses in an Al-BSF and a PERC cell is shown in Fig. 3. Thereby, we separate the remaining recombination losses into front, rear and base contributions at the different operating conditions: short-circuit, maximum power point (MPP) and open-circuit. This method has been described by *Steingrube* [20]. The different recombination fractions at different operating conditions are partially responsible for the observed fill factor. Particularly, the recombination in the base (bulk material) reaches more than 10% of the total recombination loss (see Figure 3) in the PERC cell, because the recombination losses are substantially reduced at the front and the rear side.

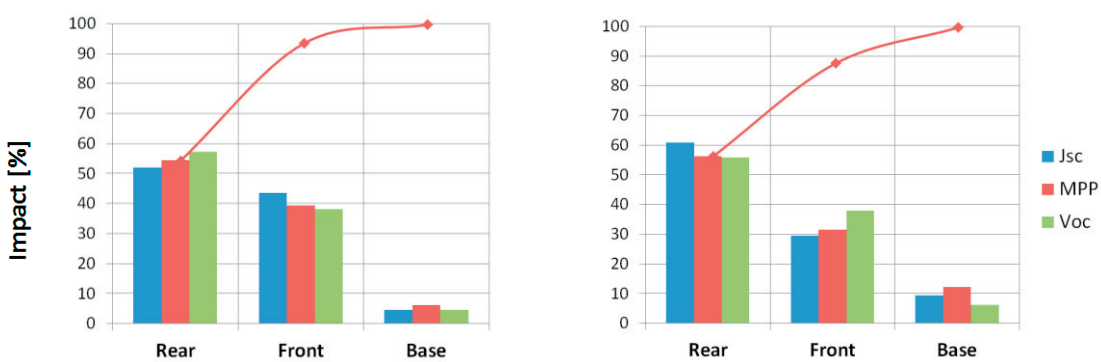

Fig. 3. Recombination loss Pareto for Al-BSF (left) and PERC (right) at the different operating points.

In order to quantify and separate the resistance and recombination loss causing the difference in the *FF* between the Al-BSF and the PERC cell we calculated also the series resistance R_s. Therefore we introduce the internal series resistance $R_{s,internal}$ which contains only contributions from the two dimensional simulation domain, i.e. spreading resistance of the bulk, emitter resistance and front and rear contact resistance. This $R_{s,internal}$ is extracted from simulations using the double light-level method according to reference [20]. Subsequently, we calculate a series resistance free fill factor (pseudo *FF*). The difference in this simulated pseudo *FF* between the Al-BSF and the PERC cell is $0.3\%_{abs}$ which is roughly one-third of the total *FF* loss between our Al-BSF and PERC cells.

4.2. Sensitivity analysis of front and rear side recombination losses

In order to understand variations in cell parameters, a sensitivity analysis has been applied to the above described 2D device model [21]. We varied the emitter saturation current density (J_{0e}) and the rear surface recombination velocity (S_{rear}). Furthermore, an inhomogeneous local BSF depth and doping density has been simulated by varying one of two contacts in the two dimensional device simulation domain. These variations have been done in a systematic, central composite Design of Experiments (DoE). Fig. 4 shows the results in terms of an "adjusted response graph", i.e. influences from other input parameters on cell parameters are corrected by setting them to their mean value. The cell parameter are "studentized" which describes the difference of the simulated value and calculated mean value divided by the calculated standard deviation.

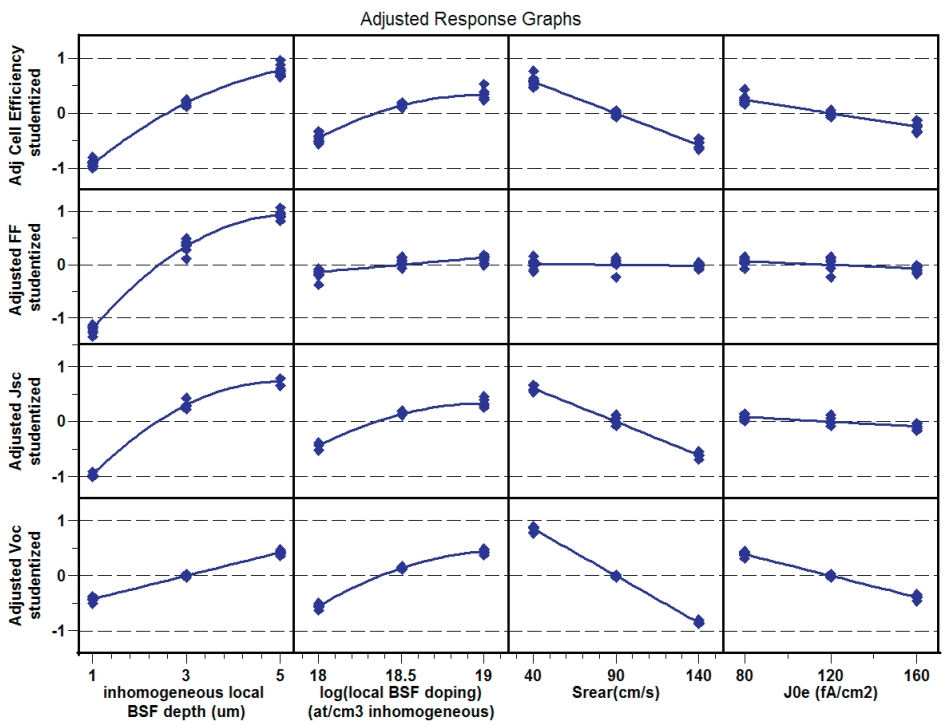

Fig. 4. Adjusted response graph for variations in the PERC device model - sensitivity analysis

The graph (Figure 4) can be interpreted in terms of how much fluctuation in an input parameter results in one standard deviation σ variation in a cell parameter. With this sensitivity analysis we are able to interpret the observed distribution of our cell parameters. It should be emphasized that besides the emitter recombination and rear recombination in the silicon and passivation layer interface, the quality of the local BSF has a strong impact on the electrical solar cell performance and its variation. In fact the *FF* is mostly influenced by the depth of the local BSF.

5. Conclusion

In this work we present the evaluation and implementation of the PERC concept in the pilot line of the SolarWorld Innovations technology center. The comparison of this cell concept with the standard Al-BSF concept reveals 1.1% absolute higher median efficiencies for the PERC design. The results of the two-dimensional simulations with Sentaurus Device show a very good agreement with the experimental data of the comparison. The observed FF difference is due to two third by the increased series resistance and one third by the injection dependent bulk recombination which is more dominating for PERC than for Al-BSF solar cells at the maximum power point. The PERC concept has been successfully tested in a high volume pilot line production over 4 weeks. We applied the statistical method of the process capability control to validate the PERC concept in terms of applicability in high volume manufacturing. Sensitivity analysis based on simulations reveals that the local BSF formation has an important impact for the solar cell performance which has been underestimated so far.

Acknowledgements

The authors would like to thank all members of the departments of the technology center, solar cell development, characterization, module development and module testing at SolarWorld Innovations in Freiberg, Germany and the research and development department of SolarWorld Industries America, USA.

We gratefully thank P.P. Altermatt for the very helpful discussions.

This work was supported by the German Federal Ministry for the Environment (BMU) under Contracts No. 0325277A (project SONNE) and No. 0325204 (project SIMPSONS).

References

[1] A. W. Blakers and A. Wang, Applied Physics Letters, vol. 55, (13), 1989, pp. 1363.

[2] Sentaurus. Synopsys, Mountain View, CA

[3] S. Gatz, J. Müller, T. Dullweber, R. Brendel, „Analysis and optimization of the bulk and rear recombination of screen-printed PERC solar cells", Energy Procedia 27 (2012) 024107

[4] U. Jäger, S. Mack, C. Wufka, A. Wolf, D. Biro, J. Nekarda, et al. „ Selective Emitters in Passivated Emitter and Rear Silicon Solar Cells Enabling 20% on Large Area p-Type Silicon", Proceedings of the 27th European Photovoltaic Solar Energy Conference and Exhibition, Frankfurt (2012)

[5] T. Lauermann, T. Lüder, S. Scholz, B. Raabe, G. Hahn, B. Terheiden, „Enabling Dielectric Rear Side Passivation for Industrial Mass Production by Developing Lean Printing-Based Solar Cell Processes", Proceedings of the 35th IEEE PV Specialists Conference, Honolulu (2010)

[6] A. Wang, J. Zhao, and M.A. Green, "24 % efficient silicon solar cells", Appl. Phys. Lett. 57 (6), 602-604 (1990).

[7] J. Schmidt, A. Merkle, R. Brendel, B. Hoex, M.C.M. van de Sanden, and W.M.M. Kessels, "Surface passivation of high-efficiency silicon solar cells by atomic-layer-deposited Al2O3", Prog. Photovolt: Res. Appl. 16 (6), 461-466 (2008).

[8] E. Schneiderlöchner, R. Preu, R. Lüdemann, S. Glunz, „Laser-fired rear contacts for crystalline silicon solar cells", Prog Photovolt 2002; 34, p. 29-34.

[9] S. Mack, U. Jäger, G. Kästner, E.A. Wotke, U. Belledin, A. Wolf et al., "Towards 19 % efficient industrial PERC devices using simultaneous front emitter and rear surface passivation by thermal oxidation", Proceedings of the 35th IEEE Photovoltaic Specialists Conference (PVSC) 2010, Honolulu, USA, 2010.

[10] B. Vermang & et al, "Integration of Al2O3 as front and rear surface passivation for large-area screen-printed p-type Si PERC," Energy Procedia vol. 27, pp325 – 329, 2012.

[11] S. Joos, U. Heß, S. Seren, B. Terheiden, G. Hahn, "Stacked PECVD backside dielectrics: An option for a firing stable passivation of industrial type screen-printed silicon solar cells" Proceedings of the 25th European Photovoltaic Solar Energy Conference and Exhibition, Valencia (2010), WIP-Renewable Energies, 2010. pp. 1875-1878

[12] P. Engelhart, D. Manger, B. Klöter, S. Hermann, A.A. Stekolnikov, S. Peters, et al., „Q.ANTUM – Q-Cells next generation high-power silicon cell & module concept", Proceedings of the 26th European Photovoltaic Solar Energy Conference and Exhibition, Hamburg (2011)

[13] A. Lachowicz, K. Ramspeck, P. Roth, M. Manole, H. Blanke, W. Hefner, et al., "NOx-Free Solution For Emitter Etch-Back", Proceedings of the 27th European Photovoltaic Solar Energy Conference and Exhibition, Frankfurt (2012)

[14] K.A. Münzer, J. Schöne, M. Hanke, M. Hein, A. Teppe, J. Maier, et al., „CENTAURUS solar cell technology in production", Proceedings of the 27th European Photovoltaic Solar Energy Conference and Exhibition, Frankfurt (2012)

[15] D.E. Kane and R.M. Swanson, "Measurement of the emitter saturation current by a contactless photoconductivity method", Proceedings of the 18th IEEE PV Specialists Conference, Las Vegas (1985), pp. 578-581

[16]] Altermatt PP. J Computational Electronics 10, 314-330 (2011)

[17] J. Schmidt, B. Lim, DK Bothe, S. Gatz, T. Dullweber, P. Altermatt; Impurity-related limitations of next-generation industrial silicon solar cells. IEEE Journal of Photovoltaics, 3 (2013), pp. 114-118.

[18] A.G. Aberle, S.J. Robinson, A. Wang, J. Zhao, S.R. Wenham, M.A. Green, Progress in Photovoltaics: Research and Applications 1, 133-143 (1993)

[19] D. Macdonald and A. Cuevas, Progress in Photovoltaics: Research and Applications 8, 362-375 (2000)

[20] S. Steingrube et al., „Loss analysis and improvements of industrially fabricated Cz-Si solar cells by means of process and device simulations" Energy Procedia 8, 263–8 (2011).

[21] G. Fischer, M. Müller, H. Wagner, S. Steingrube, P.P. Altermatt Energy Procedia 27, 203–207 (2012)

[22] F. Wolny, T. Weber, M. Müller, G. Fischer, "Light induced degradation and regeneration of high efficiency Cz PERC cells with varying base resistivity", Proceedings of the 3rd International Conference on Crystalline Silicon Photovoltaics Silicon PV 2013